Journal Pre-proof

Biosensing strategies for the detection of SARS-CoV-2 nucleic acids

Alejandro Tamborelli, Michael López Mujica, Pablo Gallay, Virginia Vaschetti, Daiana Reartes, Rocío Delpino, Leonardo Bravo, Soledad Bollo, Marcela Rodríguez, María Dolores Rubianes, Pablo Dalmasso, Gustavo Rivas

Please cite this article as: Alejandro Tamborelli, Michael López Mujica, Pablo Gallay, Virginia Vaschetti, Daiana Reartes, Rocío Delpino, Leonardo Bravo, Soledad Bollo, Marcela Rodríguez, María Dolores Rubianes, Pablo Dalmasso and Gustavo Rivas, Biosensing strategies for the detection of SARS-CoV-2 nucleic acids, *Journal of Pharmaceutical and Biomedical Analysis*, (2023) doi:https://doi.org/10.1016/j.jpba.2023.115370

This is a PDF file of an article that has undergone enhancements after acceptance, such as the addition of a cover page and metadata, and formatting for readability, but it is not yet the definitive version of record. This version will undergo additional copyediting, typesetting and review before it is published in its final form, but we are providing this version to give early visibility of the article. Please note that, during the production process, errors may be discovered which could affect the content, and all legal disclaimers that apply to the journal pertain.

Biosensing strategies for the detection of SARS-CoV-2 nucleic acids

Alejandro Tamborelli[1,2], Michael López Mujica[1], Pablo Gallay[1], Virginia Vaschetti[1,2], Daiana Reartes[1], Rocío Delpino[1], Leonardo Bravo[1], Soledad Bollo[3], Marcela Rodríguez[1], María Dolores Rubianes[1], Pablo Dalmasso[2,*], Gustavo Rivas[1,*]

[1] INFIQC, CONICET-UNC, Departamento de Fisicoquímica, Facultad de Ciencias Químicas, Universidad Nacional de Córdoba. Ciudad Universitaria, 5000 Córdoba, Argentina.

[2] CIQA, CONICET, Departamento de Ingeniería Química, Facultad Regional Córdoba, Universidad Tecnológica Nacional. Maestro López esq. Cruz Roja Argentina, 5016 Córdoba, Argentina.

[3] Advanced Center for Chronic Diseases (ACCDiS). Facultad de Ciencias Químicas y Farmacéuticas, Departamento de Química Farmacológica y Toxicológica Facultad de Ciencias Químicas y Farmacéuticas, Universidad de Chile. Sergio Livingstone 1007, Independencia, Santiago, Chile.

* Corresponding authors, e-mail addresses: pdalmasso@frc.utn.edu.ar, p-dalmasso@hotmail.com (P.R. Dalmasso); gustavo.rivas@unc.edu.ar (G.A. Rivas).

ABSTRACT

The COVID-19 pandemic had devastating effects throughout the world, producing a severe crisis in the health systems and in the economy of a long list of countries, even developed ones. Therefore, highly sensitive and selective analytical bioplatforms that allow the descentralized and fast detection of the severe acute respiratory síndrome coronavirus 2 (SARS-CoV-2), are extremely necessary. Since 2020, several reviews have been published, most of them focused on the different strategies to detect the SARS-CoV-2, either from RNA, viral proteins or host antibodies produced due to the presence of the virus. In this review, the most relevant biosensors for the detection of SARS-CoV-2 RNA are particularly addressed, with special emphasis on the discussion of the biorecognition layers and the different schemes for transducing the hybridization event.

Keywords:

COVID-19; SARS-CoV-2 RNA detection; Biosensing strategies; Genosensor.

1. SARS-CoV-2 and COVID-19 diagnosis: General aspects

The coronavirus disease (COVID-19) is produced by the Severe Acute Respiratory Syndrome Coronavirus 2 (SARS-CoV-2) reported for the first time in Wuhan, China on December 2019. This disease was responsible for one of the most terrible pandemics, with millions of people infected and dead all over

the world [1]. In fact, at 26 February 2023, the Health World Organization (WHO) has reported over 758 million confirmed cases and over 6.8 million deaths [2]. Coronaviruses belongs to the Coronidovirineae suborder under the Coronaviridae family and they are mostly zoonotic, infecting several animal species, such as camels, cats, bats, and cattle. Among them, only seven types of coronaviruses have been reported with human-to-human transmision [3,4]. In the last two decades, three coronaviruses have been responsible of human diseases, ranging from a simple cold to a severe acute respiratory sindrome (SARS). In February 2003, the SARS-related coronavirus (SARS-CoV) was first reported in Asia and then it was extended to several countries on different continents [5]. The Middle East respiratory syndrome (MERS), a viral respiratory disease caused by MERS-related coronavirus (MERS-CoV), started in September 2012 in the Arabian Peninsula [6].

The genome sequence of SARS-CoV-2 presents 96% similarity with SARSr-CoV-RaTG13 (bat SARS) and 79.5% with SARS-CoV [7]. The diameter of SARS-CoV-2 goes between 50 and 200 nm, containing positive single-stranded RNA of of ~30 kb in length that encoded for ~9860 amino acids. Structurally, the genome includes 14 open reading frames (ORFs), which encode for 27 different proteins [8,9] and it is protected by a coiled helical capsid of 10-20 nm diameter surrounded by an envelope. The two genes, *ORF1a* and *ORF1b*, encoding two autoproteolytic polyproteins involved in the replicase complex, are located on the 5′-terminus of the genome. The four main structural proteins are encoded by the genes located on the 3'-terminus, Spike (S), envelope (E), and membrane (M) proteins, and nucleocapsid (N) protein are encoded by *ORF2*, *ORF4*, *ORF5*, and *ORF9*, respectively, and represent

about one-third of the viral genome (Fig. 1). The transmembrane S glycoprotein (150 kDa) engrosses into the viral envelope and presents protruding peplomers that give the typical and well-known crown-like appearance. The interaction with the cell is produced by the attachment of S protein that is cleaved by host cell protease, generating two non-covalently attached functional subunits [10]. S1 subunit is a receptor binding domain (RBD) and is responsable for the cellular tropism in several host virus range, while the S2 subunit is responsable of the fusion with the cell membrane [11,12]. The spike proteins are strongly attracted toward angiotensin converting enzyme 2 (ACE2) receptors, predominantly expressed in the pulmonary epithelium, which facilitate the binding of the S protein to host cells. After the viral RNA reaches the nucleus, it replicates and generates negative-strand RNA from a single-strand positive RNA template using RNA polymerase. This negative-strand RNA also helps make new positive-strand RNAs that serve as blueprints for synthesizing new viral proteins and creating new viral particles which are released into the other cells [13,14].
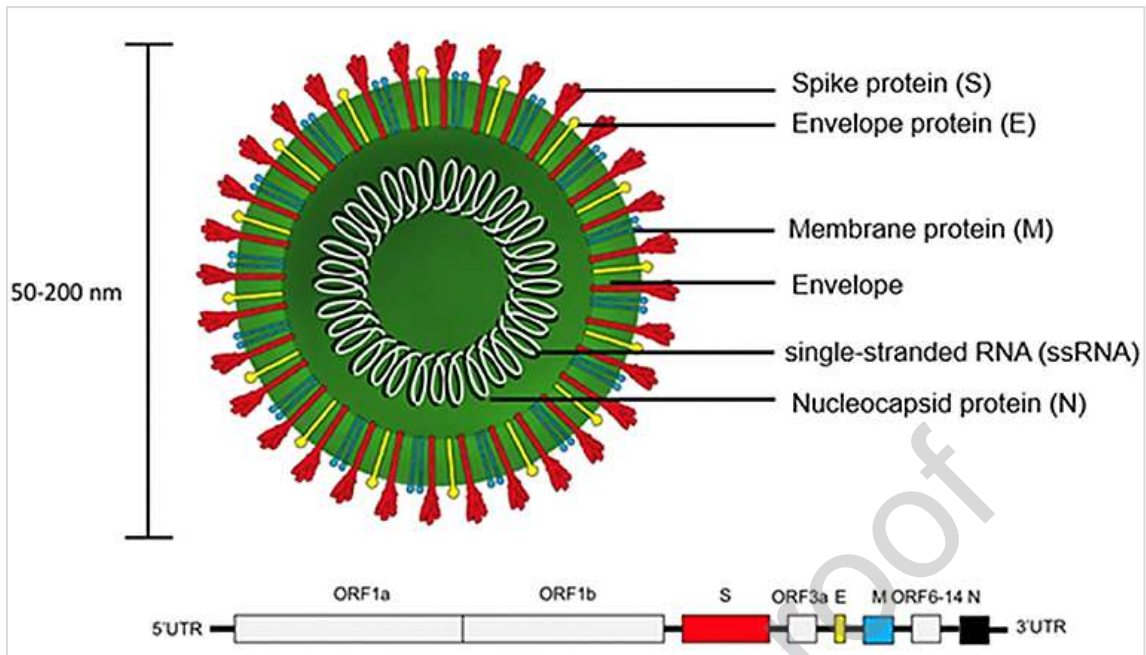
Fig. 1. Schematic representation of the structure of SARS-CoV-2 and the genomic organization. Reprinted from Ref. [4], Copyright (2021), Sharma, Kontodimas, and Bosmann, with distribution under the terms of the Creative Commons Attribution License (CC BY).

The diagnosis of COVID-19 is mainly carried out by detection of the SARS-CoV-2 viral genetic material. The preferred targets for SARS-CoV-2 gene-based analysis involves envelope (*E*) protein gene, nucleocapsid (*N*) protein gene, RNA-dependent RNA polymerase (*RdRp*) gene, and open reading frame 1a and 1b (*ORF1ab)* gene, being the *E* and *ORF1ab* genes the most commonly used for detecting SARS-CoV-2 infections [15]. The gold standard for the diagnosis of COVID-19 is the real-time reverse-transcription-based polymerase chain reaction (RT-PCR). Although this assay is highly specific and sensitive, it presents some drawbacks like the requirement of trained personnel, temperature cycling, time consuming, and the limited utility in distant and resource-constrained surroundings [16,17]. As it was extensively

discussed in several reviews, the isothermal amplification approaches are the best options because they can be operated at a single temperature without particular laboratory apparatus requirements and provide sensitive results, [18-24]. Loop-mediated isothermal amplification (LAMP) method, reverse transcription-LAMP (RT-LAMP) approach, rolling circle amplification (RCA), recombinase polymerase amplification (RPA), strand displacement amplification (SDA), NASBA (nucleic acid sequence-based amplification), and clustered regularly interspaced short palindromic repeats (CRISPR) technology have been successfully used . Currently, RT-PCR kits are replaced by RT-LAMP because it allows to detect SARS-CoV-2 in few minutes, without RNA isolation from swabs, and under sustainable conditions of pH and temperature [25,26].

As soon as the SARS.CoV-2 started to be disseminated around the world, different strategies emerged for the diagnostic of COVID-19. In fact, the detection of the viral RNA by RT-PCR was the first diagnostic tool, then complemented by the immunoassays for the quantification of immunoglobulins. The development of the antigen test, based on the detection of viral proteins, largely contributed to a faster diagnostic of positive cases in spite of the poor sensitivity compared to the RT-PCR. In the last years, several reviews summarized the different alternatives for the detection of i) SARS-CoV-2 RNA, ii) viral proteins, and iii) host antibodies produced as a consequence of the presence of the virus [18-23]. A critical discussion about these strategies, with special emphasis on the fundamentals of the different approaches for both lateral flow biosensors and nucleic acid amplification techniques (NAATs), as well as the most relevant contributions, have been reported by Rubio-Monterde et al. [19]. Tessaro et al. [20] summarized the progress in colorimetric

biosensors for detecting SARS-CoV-2, the advantages of using nanomaterials, and the application of biosensors to point-of-care (POC) diagnostic devices with special emphasis on the importance of lateral flow immunoassays. Filchakova et al. [21] presented an overview of the commercialized RT-PCR methods while Oishee et al. [22] reported an up-to-date of the FDA-approved RT-PCR and immunoassay-based kits for the detection of SARS-CoV-2, with a critical comparison of their analytical performances. Mostafa et al. [23] reported a comprehensive overview of the different strategies for the detection of SARSCoV-2 according to the target biomolecule and the technique used for the quantification, with an interesting discussion about the effect of the different mutations. Here, we provide a comprehensive review particularly focused on the most relevant biosensors developed for the detection/quantfication of SARS-CoV-2 RNA, with special emphasis on the discussion of the biorecognition layers and the transduction of the hybridization event.

2. Biosensing strategies for the detection of SARS-CoV-2

Biosensing platforms have demonstrated to be extremely useful for the detection of different molecules and, in particular, nucleic acids. They offer the alternative to make posible a quantitative analysis in short time without the requirement of sofisticated equipments, trained personal or tedious sample pretreatment, with the important advantage of the application for point-of-care (POC) measurements [27]. In the following sections and Table 1, we present the most significant contributions performed in the last three years (2020-2022) on biosensing strategies used to detect SARS-CoV-2 nucleic acid.

*2.1. Biosensing with electrochemical transduction*

Cajigas et al. [28] described a SARS-CoV-2 RNA genosensor based on a sandwich hybridization scheme, using a thiol-reactive capture probe linked to maleimide-functionalized magnetic beads as biorecognition platform, and a biotinylated signaling probe tagged with enzymatic complexes based on streptavidin-horseradish peroxidase (HRP) conjugates, which in the presence of hydrogen peroxide and tetramethyl benzidine (TMB) generates the analytical signal (Fig. 2). They proposed two transduction strategies, by spectrophotometry at 620 nm, from the absorption of the TMB oxidized product, and by electrochemistry, through the reduction of this product at -150 mV. The highest sensitivity was obtained using the probe that targets the H-conserved region of SARS-CoV-2 RNA and the streptavidin-poly-HRP80 conjugate, reaching a detection limit of 0.6 pM, that is 100 lower than the one obtained when using streptavidin-HRP. The electrochemical genosensor demonstrated the ability to detect SARS-CoV-2 and discriminate it against homologous viruses in spiked samples and samples from SARS-CoV-2 cell cultures. **López Mujica et al.** [29] proposed two biosensors for the quantification of SARS-CoV-2 nucleic acid using glassy carbon electrodes (GCE) modified with avidin (Av)-functionalized multi-walled carbon nanotubes (MWCNTs), one of them based on the impedimetric transduction through the increment of $[Fe(CN)_6]^{3-}$/$[Fe(CN)_6]^{4-}$ charge transfer resistance, and the other one, based on a sandwich hybridization scheme and amperometric transduction using HRP/hydroquinone/hydrogen peroxide. In both cases, the response was highly

selective with detection limits at aM levels. The potential analytical application of the proposed sensors was demonstrated, as a proof-of-concept using highly diluted-RT-PCR amplified SARS-CoV-2 RNA samples, with successful response even after 10^{10} times dilution. **Pina-Coronado et al.** [30] proposed the non-amplified detection of SARS-CoV-2 RNA based on the combination of two kind of nanomaterials, carbon dots functionalized with methylene blue (MB) as redox indicator, and a mixture of gold nanoparticles (AuNPs) and gold nanotriangles (AuNTs) sprayed on the screen-printed gold electrode (SPAuE) as platform for the immobilization of the thiolated DNA probe. The analytical signal was obtained by differential pulse voltammetry (DPV) from the increment of the oxidation peak current of the accumulated MB. No interference was reported in the presence of RNAs corresponding to other viruses or a single nucleotide polymorphism. The practical usefulness was demonstrated with nasopharyngeal samples from COVID-19 patients. The use of screen-printed carbon electrodes (SPCE) modified with boron nitride quantum dots (BNQDs) and flower-like gold nanostructures (FGNs) as anchoring site for a thiolated DNA probe specific for SARS-CoV-2 RNA, was proposed by **Hatamluyi et al.** [31 ~~22~~]. In this case, the hybridization event was evidenced by DPV from the decrease in the peak current of $[Fe(CN)_6]^{3-}/[Fe(CN)_6]^{4-}$ due to the electrostatic repulsion (turn-off detection strategy), and the increment of MB peak current due to its intercalation in the double helix (turn-on detection strategy) (Fig. 3). There was a linear dependence with the logarithm of the target concentration from 1.0×10^{-18} to 1.0×10^{-9} M in both cases, with a detection limit of 0.27 aM for the turn-on method. The applicability of the biosensor for clinical trials was demonstrated using RNA sequences extracted from clinical nasopharyngeal

9

swab specimens (positive and negative SARS-CoV-2 samples confirmed by RT-PCR) and even after $1:10^7$ dilution, the response of the biosensor was successful (Fig. 4).
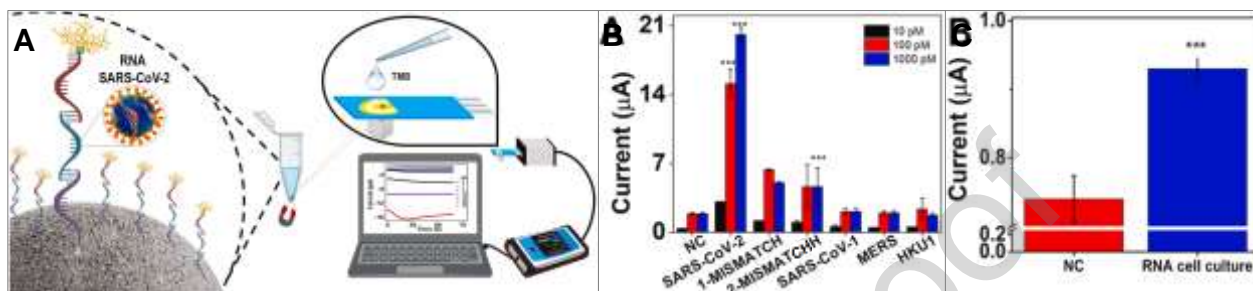

Fig. 2. (A) Schematic representation of the SARS-CoV-2 RNA detection using an electrochemical genosensor based on a sandwich hybridization scheme and chronoamperometry to obtain the analytical signal. (B) Specificity evaluation against one and two base pair mismatches from conserved sequences of SARS-CoV-2 and SARS-CoV, MERS, and HKU1 homologous counterparts at three different loads from 10 to 1000 pM. (C) Genosensor response against a positive SARS-CoV-2 RNA cell culture sample compared with a negative control (NC). Adapted from Ref. [28], Copyright (2022), with permission from Elsevier.
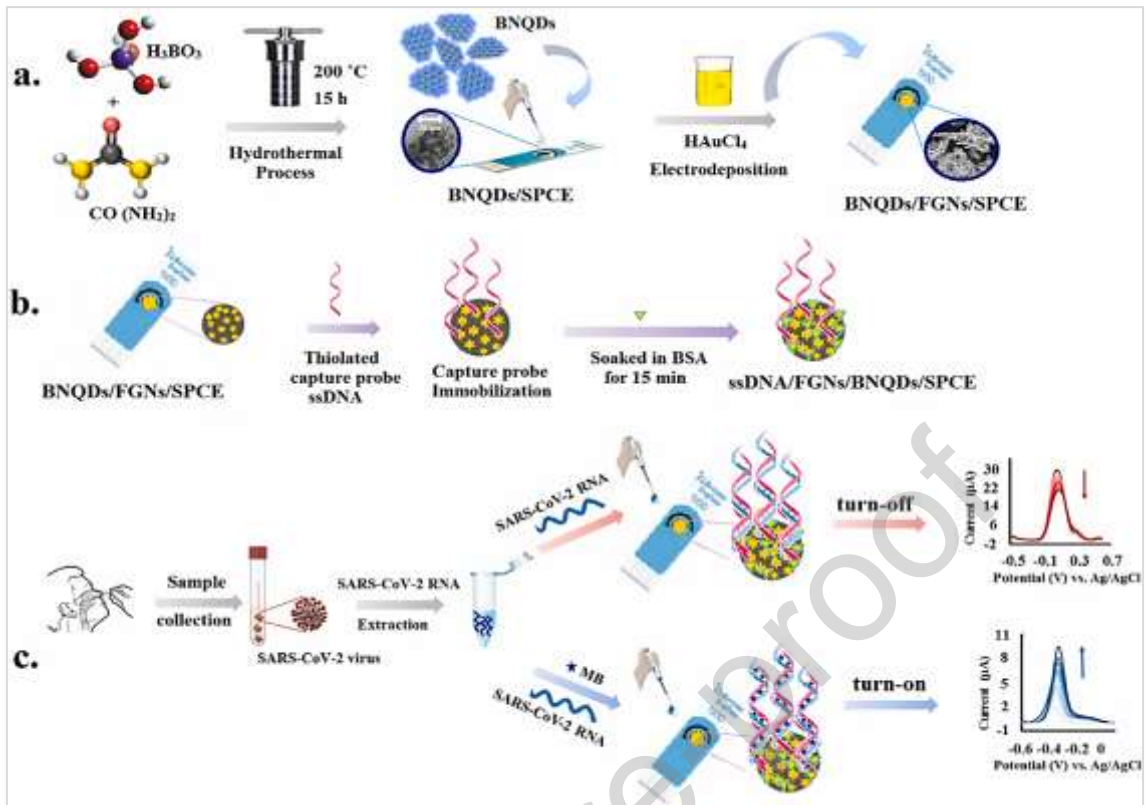
Fig. 3. Schematic representation of the SARS-CoV-2 detection using ssDNA/BNQDs/FGNs/SPCE as electrochemical biosensor. (a) Synthesis of nanostructures. (b) Capture probe immobilization and electrode preparation. (c) Process of electrochemical detection using turn-off and turn-on strategies. Reprinted from Ref. [31], Copyright (2022), with permission from Elsevier.

Alafeef et al. [32] developed a low-cost, amplification free, and easy-to-implement graphene-based electrochemical biosensor for the detection of SARS-CoV-2 RNA using a micro-Au electrode immobilized at a filter paper coated with a graphene suspension and AuNPs capped with four probes (P) that target different regions of the viral nucleocapsid phosphoprotein *N* gene thiolated at 5′ (P1 and P3) or 3′ (P2 and P4) ends. A highly sensitive analytical signal was obtained from the output voltage with a detection limit of 6.9 copies/µL and interference free detection in the presence of SARS-CoV and

MERS-CoV RNA, or negative COVID-19 samples collected from healthy subjects.
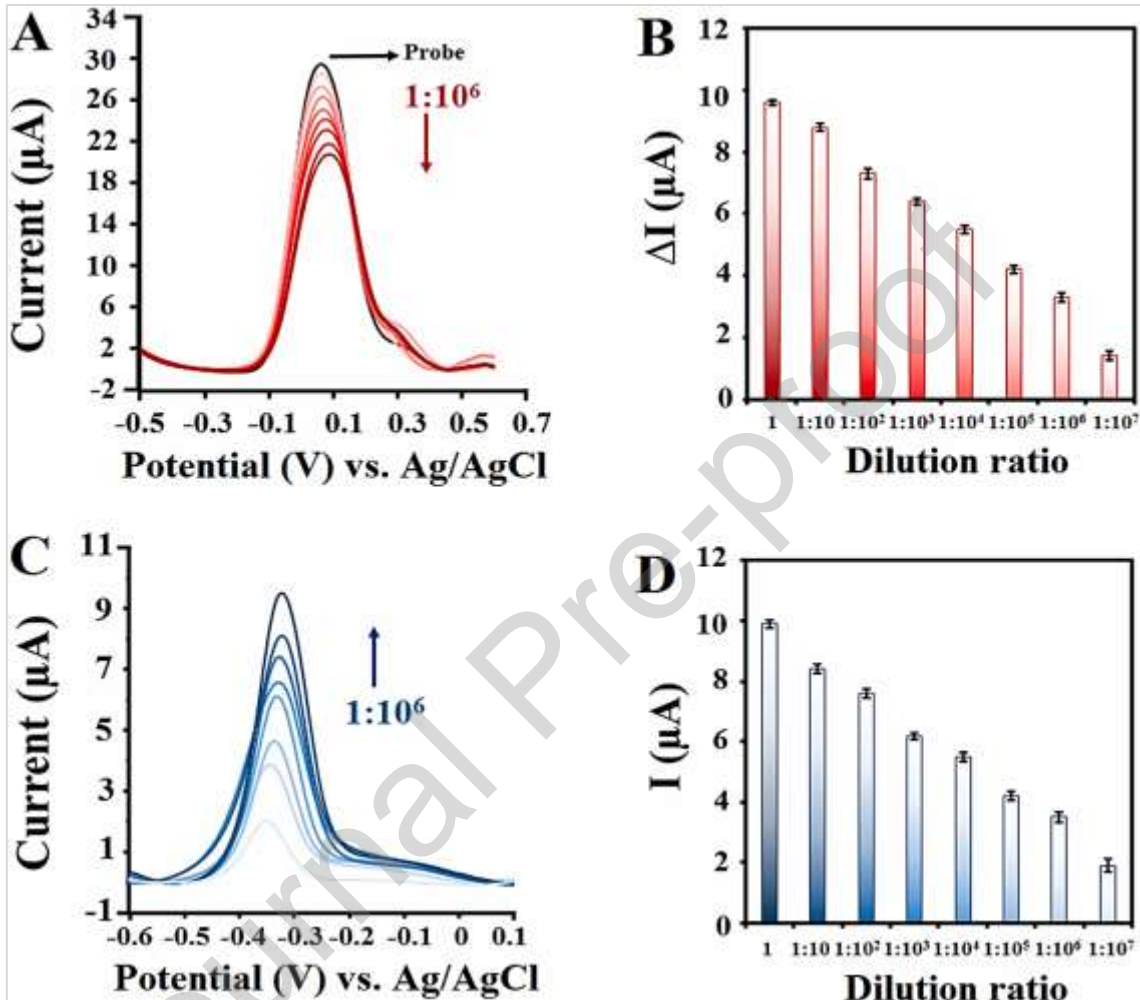
Fig. 4. DPV signals and corresponding current intensities at ssDNA/BNQDs/FGNs/SPCE for SARS-CoV-2 RNA extracted from three positive patient (cycle threshold = 20) with different dilution ratios based on turn-off (A), (B) and turn-on (C), (D) strategies. Reprinted from Ref. [31], Copyright (2022), with permission from Elsevier.

Paulose et al. [33] proposed an electrical double layer (EDL)-gated field effect transistor-based biosensor (BioFET) for the successful detection of SARS-CoV-

2 RNA from the post-hybridization electrical redistribution in the EDL capacitance and the resulting change of FET drain current. The sensor was used to rapidly detect SARS-CoV-2 *N* gene RNA in diluted human saliva at concentrations ranging from 1 fM to 1 pM. One aspect important to remark is that the EDL-gated BioFET showed similar performance in the presence of a viral envelope lysis detergent and a RNase-inactive reagent. **Deng et al.** [34] reported a target-triggered cascade signal amplification strategy to the detection of the SARS-CoV-2 *RdRp* gene through the integration of the catalytic hairpin assembly (CHA), a typical non-enzymatic nucleic acid circuit used for signal amplification with low background, and the polimerization ability of the terminal deoxynucleotidyl transferase (TdT), a kind of template-free DNA polymerase used to elongate the single strand DNA by catalyzing the addition of deoxynucleotides to the free 3′-terminus of DNA. In the presence of SARS-CoV-2 RNA, the CHA reaction generates on the electrode surface a large number of nucleic acid duplexes with free 3' –OH terminus along with the release of the target that triggers the multicycle hybridization, producing amounts of duplexes, and generating long-strand DNA after the addition of TdT. The analytical signal was obtained from the DPV signal of $[Ru(NH_3)_6]^{3+}$ electrostatically accumulated at the duplexes, with a linear range between 0.1 pM and 3000 pM, and a detection limit of 45 fM. Moreover, the proposed biosensor was successfully used for the SARS CoV-2 RNA detection in the presence of mismatched sequences and in oropharyngeal swab simples, allowing to distinguish COVID-19 patients from healthy individuals. Using a similar scheme, **Peng et al.** [35] fabricated an electrochemical genosensor for the quantification of a 26-nt-long *ORF1ab* fragment of SARS-CoV-2 RNA (which has been demonstrated to be a

13

highly conserved region) by combining the signal amplification capabilities of CHA and TdT. As in [34], the target triggers CHA to generate a double-stranded product forming a Y-shaped structure with three protruding 3′ -end, which can be elongated by TdT to form long single-stranded DNA products, able to accumulate $[Ru(NH_3)_6]^{3+}$. The linear range was more restricted than in [34] (0.1 to 1000 pM *versus* 0.1 to 3000 pM) while the detection limit was slightly lower (26 fM *versus* 45 fM). The biosensor showed very good recoveries of the spiked target RNA in serum and saliva samples as well as clinical application in oropharyngeal swabs from healthy and COVID-19 patients.

A very interesting and innovative strategy for the non-amplified detection of SARS-CoV-2 RNA was proposed by **Ji et al.** [36], who reported the detection of SARS-CoV-2 RNA by using a self-actuator molecular-electrochemical system (MECS) inspired by the hydra. This hydra-like structure consisted of a tentacle and an upstanding trunk as a prop unit. The trunk is a regular tetrahedral structure with four double-stranded DNAs that intertwine to form edges bound through amino groups to the pyrenebutanoic acid succinimidylester-treated graphene electrode. The tentacle is a flexible single-stranded DNA that extends from the top vertex of the tetrahedral trunk and contains the probe that recognizes the *ORF1ab* gene of SARSCoV-2 RNA with five thymine units that allow the free-movement of the tentacle after target recognition, and MB at the top as the electrochemical label (Fig. 5). The tentacle remains upright spontaneously in the local electrical field on the graphene surface due to the negative charges on the ss-DNA backbones, and once the hybridization takes place, the tentacle and the nearby labels move downward spontaneously to the vicinity of the interface due to the steric effect

as well as the electrostatic force generated by the negative charges of the target. Two important advantages of MECS are that it enables direct testing of unamplified clinical samples, and that it is posible to detect 4 copies of SARS-CoV-2 RNA in 80 μL artificial saliva, representing a very competitive detection limit.
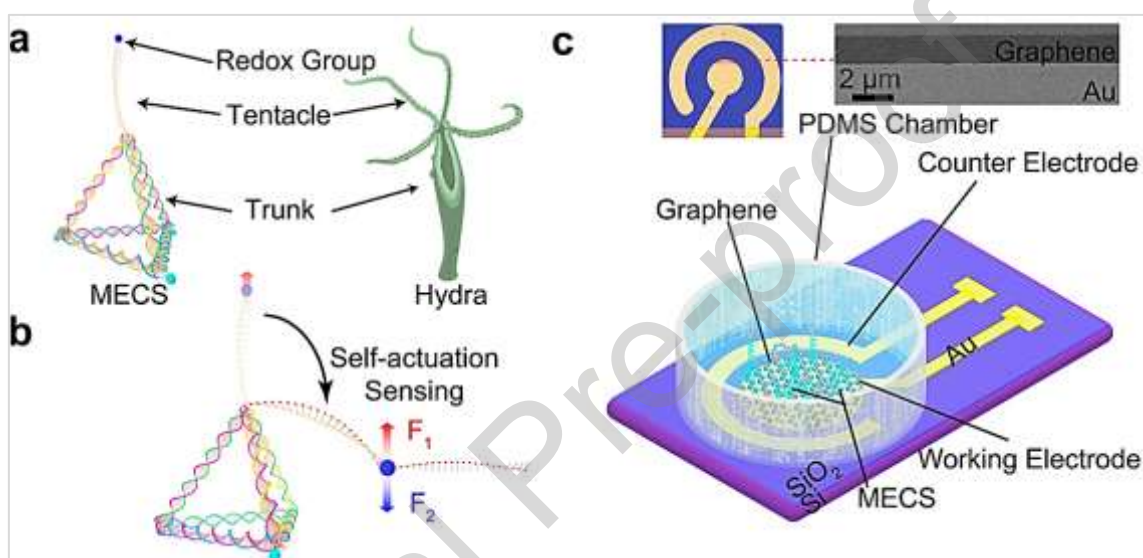
Fig. 5. Electrochemical detection of unamplified SARS-CoV-2 RNA using a MECS-modified graphene microelectrode. (a) Structure of the proposed MECS based on DNA nanostructures that mimic the hydra architecture. (b) Schematic illustration of MECS for the RNA sensing process: F1 represents the upward repulsion force of the local electric field that pulls the tentacle away from the electrode, and F2 represents the downward driving forces and steric effects that actuate the tentacle close to the electrode. (c) Device configuration of the MECS-modified graphene microelectrode (inset: optical microscope image of the working electrode and SEM image of graphene). Adapted with permission from Ref. [36]. Copyright (2022) American Chemical Society.

In overview, the electrochemical biosensors represent interesting and cost-effective alternatives for the quantification of SARS-CoV-2 RNA in a very simple and fast way, with the great advantage that the prior RNA- or signal-amplification step is not always required, at variance with the well known RT-PCR or the isothermal amplification techniques. On the other hand, some of them have remarkable analytical performances, that make them really competitive compared to the classical molecular detection techniques.

2.2. Biosensing with electrochemiluminescent transduction

Fan et al. [37] reported an enzyme-free entropy-driven reaction amplified electrochemiluminescence (ECL) strategy to detect *RdRp* gene at fM level with successful application in human serum samples. The biorecognition layer was built at a gold electrode and consisted of a rigid DNA tetrahedron which contains the probe in the vertex and this scaffold makes posible that the target-participated entropy-driven amplified reaction occurs and efficiently propiciate the link of the $[Ru(bpy)_3]^{2+}$ modified DNA to the linear ssDNA at the vertex of the tetrahedron to give the ECL. **Yin et al.** [38] proposed a dual wavelength ratiometric ECL genosensor for the ultrasensitive detection of the SARS-CoV-2 *RdRp* gene based on resonance energy transfer (RET) between graphitic carbon nitride nanosheets (g-C_3N_4) and Ru-SiO_2 nanospheres functionalized with folic acid (Ru-SiO_2@FA), using a bipedal three-dimensional (3D) DNA walker amplification strategy (Fig. 6). The sensor was prepared by dropping a g-C_3N_4 suspension on top of a gold electrode followed by the addition of a highly rigid structure of triple-helix DNA (tsDNA), which was

16

incubated to make it stand upright on the surface of g-C_3N_4 due to the affinity of the ssDNA tail with graphitic carbon nitride and the poor affinity of the triple-helix, exposing the probe sequence. In this way, trace amounts of target genes were converted to a large number of output DNAs by 3D DNA walker multiple amplification. The output bridged a multifunctional probe Ru-SiO_2@FA to the electrode producing ECL RET from the gC_3N_4 to Ru-SiO_2@FA, with the consequent decrease of the ECL signal at 460 nm, due to the quenching produced by Ru-SiO_2 and FA, and the increase of ECL at 620 nm due to Ru-SiO_2. The ECL_{620}/ECL_{460} ratio was used as analytical signal and the biosensor showed an excellent sensitivity for *RdRp* gene with a linear range between 1 fM and 10 nM, a subfM detection limit, and experimental recovery ranges from 92% to 102.1% for different concentrations of *RdRp* gene mixed with healthy human throat swab samples. Following a similar scheme, **Fan et al.** [39] proposed a biosensor based on the combination of entropy-driven and bipedal DNA walker cycle amplification that consists of a tetrahedron immobilized at a gold electrode modified with Au-g-C_3N_4 for the dual-wavelength ratiometric ECL detection of the *RdRp* gene of SARS-CoV-2 at aM level. The entropy-driven cyclic amplification reaction was started by the SARS-CoV-2 *RdRp* gene to generate a bandage that combines with the two feet of the bipedal DNA walker (ssDNAs) to form a bipedal DNA walker and create the next cycle reaction. Once completing the walking process, and in the presence of the Nb.BbvCl endonuclease, a synthesized PEI-Ru@Ti_3C_2@AuNPs-thiolated DNA(S7) probe was combined with the excised hairpin part of DNA tetrahedrons, generating the expected decrease of the ECL at 460 nm and an increment of the ECL at 620

17

nm. In contrast to the rest of SARS-CoV-2 RNA biosensors, this one was challenged with a 50 fold diluted human serum.
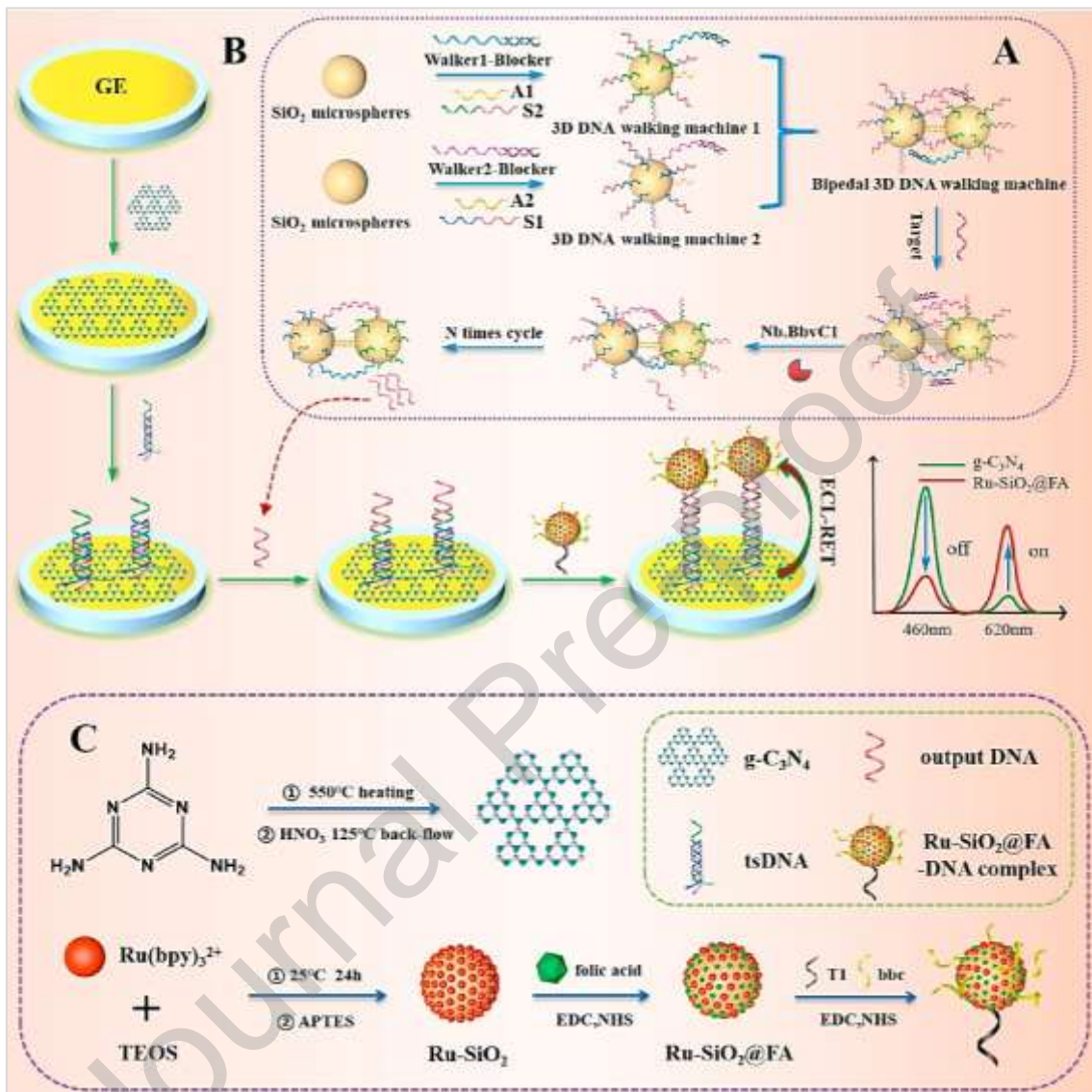
Fig. 6. Schematic illustration of a dual-wavelength ratiometric ECL biosensor based on RET platform of g-C$_3$N$_4$ nanosheets and Ru–SiO$_2$@FA for detection of *RdRp* gene. Reprinted from Ref. [38], Copyright (2022), with permission from Elsevier.

Also in the same direction of the previous biosensors, **Zhang et al.** [40] reported a ratiometric ECL biosensor for the detection at aM level of *RdRp* gene

and its successful application in human pharyngeal swabs, based on the use of a GCE modified with AuNPs-g-C$_3$N$_4$ and a three-stranded Y-type DNA (Y-DNA) as probe. The target triggered the hybridization chain reaction (HCR) and allowed the association of a Ru-modified DNA, with the consequent increase of the ECL at 620 nm and the decrease at 460 nm. **Zhang et al.** [41] proposed a biosensor for the detection of *RdRp* gene at aM level through the combination of 3D DNA walker amplification scheme and detection based on the activity of CRISPR-associated endonuclease Cas12a (CRISPR-Cas12a) and ECL transduction. In the first part, the nano-machine mainly contains a DNA-modified AuNP (DNA-AuNP), a walking leg, and a fuel. The DNA-AuNP is a conjugate with a three-stranded substrate complex (DNA1/DNA2/DNA3) and an affinity ligand (DNA4) on a single AuNP. The cleavage activity of CRISPR-Cas12a was activated by the amplification product double-stranded DNA, which could indiscriminately cut the single-stranded DNA on the surface of a MXene based ECL material (PEI-Ru@Ti$_3$C$_2$@AuNPs-DNA) as sensor, and caused the ferrocene modified at one end of the DNA to move away from the electrode surface, increasing the ECL signal with a detection limit of 12.8 aM.

Electrochemiluminescent biosensors offer a very interesting alternative for the highly sensitive detection of SARS-CoV-2 nucleic acid, although the approaches are more limited than the electrochemical ones due to the special requirement of the system to generate the electroluminescent signal.

2.3. Biosensing with optical transduction

Xie et al. [42] proposed a biosensor called CRISPR-CNS (cost-effective, nimble, and sensitive copper nanocluster sensor integrating CRISPR) by developing a label-free and low-background reporter for CRISPR/Cas12a signaling through the integration of the DNA-templated copper nanoclusters (DNA-CuNCs) and exonuclease I (EXO I). The template of the DNA-CuNCs was rationally designed as a ds-/ss-DNA hybrid, ensuring that after a quick and nonpersistent cut of Cas12a, a majority of the template can be digested by EXO I. Due to the high signal-to-background ratio of the proposed reporter, CRISPR-CNS shows excellent performances for nucleic acid detection, yielding a detection limit of 20 copies of SARS-CoV-2 RNA. **Ma et al.** [43] proposed two strategies for the detection of SARS-CoV-2 RNA after reverse transcription and amplification using specific primers for SARS-CoV-2 gene to obtain dsDNA amplicons (target DNA). In one case, the biosensor was based on the change of the color of AuNPs due to the disaggregation produced after cutting the ssDNA that stabilized them by the action of CRISPR-Cas12a. This color change could be detected by naked eyes or using a smartphone readout with Color Picker App. The proposed biosensor was successfully used to detect SARS-CoV-2 gene in a fast way (90 min) in synthetic vectors, transcribed RNA, SARS-CoV-2 pseudoviruses, and clinical biosamples, allowing the detection of 1 copy/µL with no cross-reactivity. The other strategy was based on the increase of fluorescence due to the dequenching produced after the *trans*-cleavage activity of Cas-12a that broke the close vicinity between a fluorophore at 5′ and a quencher at 3' ends in a doubly labeled ssDNA. This strategy also made it possible the detection of 1 copy/µL. **Huang et al.** [44] reported a very interesting biosensor able to be used for POC applications. In fact, they

20

proposed the portable, rapid, and sensitive (10 copies/μL) detection of the *N* gene of SARS-CoV-2 based on the use of CRISPR Cas12a. The swab samples were treated by lysis and the released RNA was amplified by reverse transcription recombinase-aided amplification (RT-RAA), generating complementary dsDNA. In CRISPR RNA (crRNA), Cas12a specifically recognizes the amplified DNA (target) and exhibits its ssDNA cleavage activity, releasing the ssDNA-conjugated invertase on magnetic beads (MBs), which in the presence of sucrose catalyzes its hydrolysis into fructose and glucose. In this way, the glucose can be determined witn a personal glucose meter (PGM) (Fig. 7). This PGM-CRISPR assay allowed the *N* gene detection in the range of 10^1-10^4 copies/μL, which was acceptable for early diagnosis. Moreover, the authors challenged the sensor with samples of patients with COVID-19, healthy persons, and patients infected with other viruses. They also used throat swabs samples from healthy volunteers enriched with *N* gene segments of SARS-CoV.
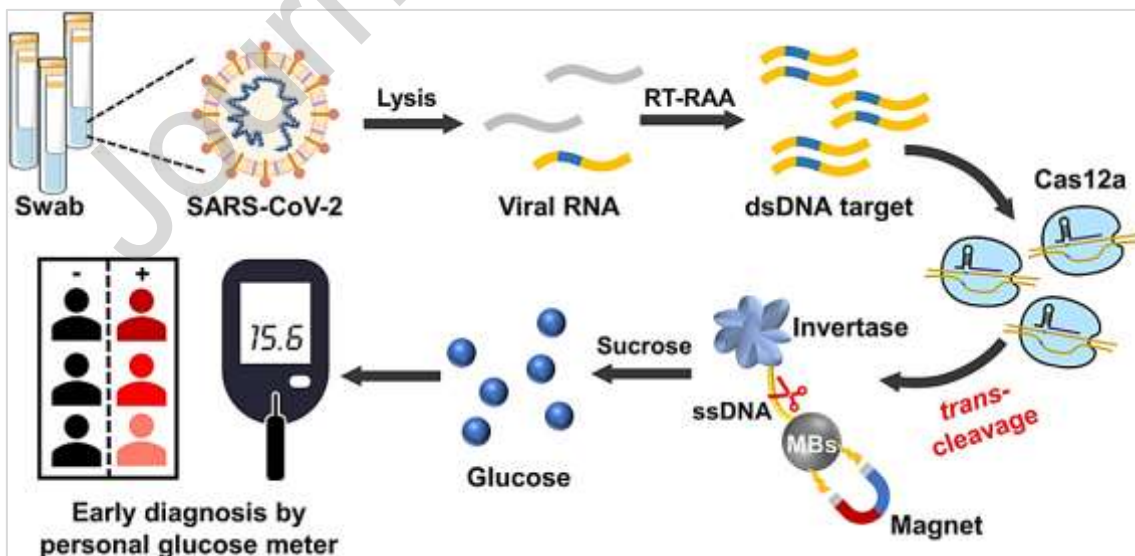
Fig. 7. Working principle of CRISPR Cas12a-derived biosensor enabling portable personal glucose meter readout for quantitative detection of SARS-

CoV-2. Reprinted from Ref. [44], Copyright (2021), with permission from John Wiley and Sons.

Liang et al. [45] proposed an amplification-free CRISPR/Cas12a-based detection of the reverse transcribed product of SARS-CoV-2 RNA gene at fM level with SERS transduction, called SERS-CRISPR. The SERS probe was obtained by mixing MBs modified with streptavidin and biotinylated-ssDNA-HS, and AgNPs@4-ATP (4-aminothiophenol). The analytical signal was obtained from the Raman peak (1074 cm^{-1}) of 4-ATP and the biosensor was used to detect SARS-CoV-2 derived nucleic acids in RNA extracts obtained from nasopharyngeal swab samples. **López-Valls et al.** [46] presented a sensing system called CASCADE (CRISPR/CAS-based Colorimetric nucleic Acid Detection) for the fast and specific naked-eye detection of SARS-CoV-2 RNA. When the target RNA was specifically recognized by the CRISPR-associated endonuclease LwaCas13 (CRISPR-Cas13a), it activated its collateral RNase activity and cleaved ssRNA conjugated to AuNPs. After enzymatic degradation, the AuNPs cannot be stabilized since the short oligonucleotides cannot cover the entire AuNP surface, producing their aggregation. The change of color after aggregation is used as analytical signal, allowing the detection at pM level. An additional decrease in the detection limit to fM or even aM level, was reached coupling CASCADE to isothermal nucleic acid amplifications, such as RPA and NASBA, respectively. The biosensor was successful in detecting SARS-CoV-2 in clinical samples from nasopharyngeal swabs. **Mahas et al.** [47] introduced a new Cas13 variant, called miniature Cas13 (mCas13), and proposed a SARS-CoV-2 RNA biosensor through the association of RT-LAMP and Cas13 to make

22

posible a fast, accurate, simple, and cost-effective biosensing methodology for the detection of SARS-CoV-2 RNA in synthetic and clinical samples. Moreover, they adapted a handheld fluorescence visualizer for the mCas13-based visual detection with the human eye without the need for sophisticated instruments like qPCR machines.

Qin et al. [48] reported the label free detection of SARS-CoV-2 *N* gene through the use of a molecular beacon specifically designed to recognize the viral RNA based on the use of human telomeric guanine-triplex (ht-G3), which lights up Thioflavin T (ThT). This molecular beacon consists of three fragments, an ht-G3 sequence at the 3' end, a loop that recognizes the target, and a sequence at the 5' end complementary to part of the G3 sequence. After target addition, the region of the loop binds to the target to form the DNA-RNA double helix, opening the stem region to release the G3 sequence. In the presence of an optimized concentration of K^+, the reduplicated TTAGGG of the telomerase self-assembled into a G3 structure. The introduction of (duplex specific nuclease) (DSN), enzyme that cuts DNA-DNA or RNA-DNA duplexes, destroyed the DNA segment with RNA target, releasing the target to recycle. After addition of ThT, there was an increment in the fluorescence promoted by ht-G3, allowing the detection of 0.01 nM of viral RNA, which was 100 times lower than the one obtained in the absence of DSN. Borghei et al. [49] proposed a naked-eye, label-free, and RNA extraction-free colorimetric method for the direct detection of *N* gene of SARS-CoV-2, based on the use of 4 antisense oligonucleotides (ASOs) of 20 bases modified with a polyG tail of 12 units at the 5' end of ASO_1 and ASO_3, and at the 3' end of ASO_2 and ASO_4, as a template for *in situ* formation of anisotropic AuNPs without any chemical

23

modification or DNA labeling (ASOs@AuNPs) (Fig. 8). After hybridization with the viral target RNA, there was a red shift in the localized surface plasmon resonance and the color of the solution changed from red to purple due to the aggregation of the AuNPs. The performance of this method was evaluated directly on throat samples without RNA extraction, which agreed satisfactorily with the results obtained for the SARS-CoV-2 samples tested by RT-qPCR for *N* gene.
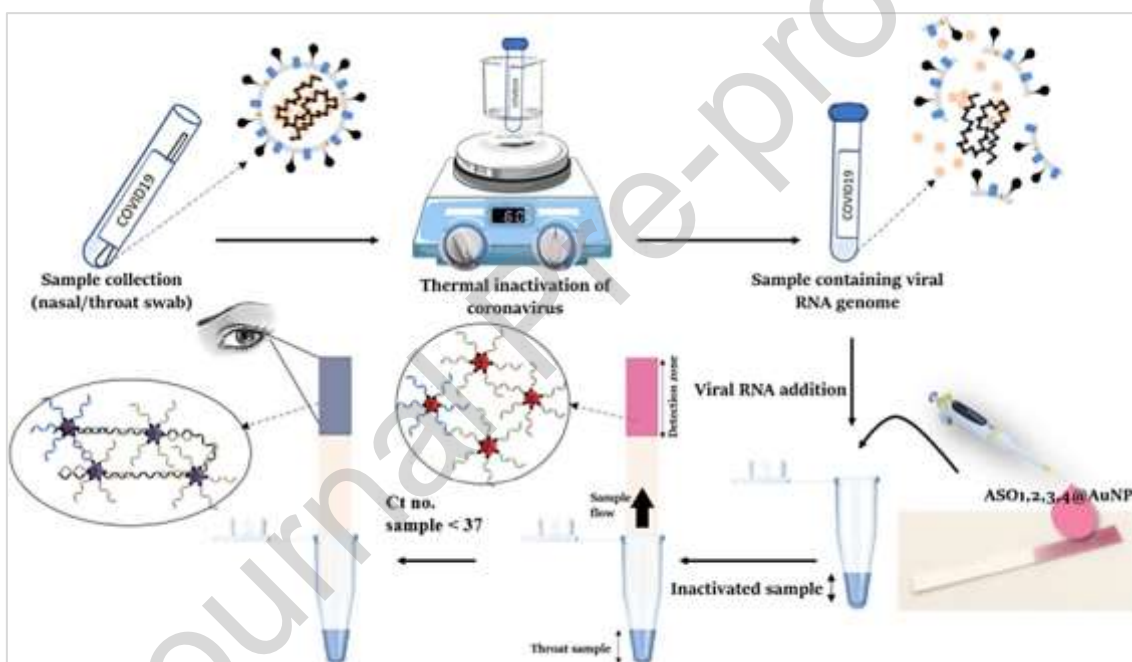
Fig. 8. Schematic representation of the ASOs@AuNPs-based colorimetric assay for the SARS-CoV-2 *N* gene detection. Reprint with permission from Ref. [49]. Copyright (2022) American Chemical Society.

2.4. Lateral flow biosensing

Lateral flow (LF) biosensors present the advantages of being portable, simple, low-cost, without requirement of batteries or equipments, characteristics

that make them very attractive for POC measurements, low-resource settings, and emergency use [19,50,51]. The application field is very broad, involving environmental and food control, veterinary and medicine. A commercially available LF strip present four basic components: a sample pad, a conjugate pad, a nitrocellulose membrane (that contains the test line and the control line), and an absorption pad. The sample is added in the sample pad and by capillary it reaches the conjugate pad where there is a bioreceptor immobilized at the NPs. If the target is present, it will be recognized by the specific receptor and the positive result will be indicated by a color line (the test line (TL)). The sample continues through the detection pad and a control line (CL), containing a secondary bioreceptor, should appear for all valid tests. An absorption pad located at the end of the strip absorbs the fluid excess. The bioreceptor can be an antibody, a nucleic acid probe, or an aptamer, depending on the target. AuNPs are the most used nanomaterial in LF tests due to their high biocompatibility that makes possible the conjugation with the bioreceptors, their reproducible synthesis, tuneability, and drastic changes of color depending on the aggregation state [19,50,51]. Even though LF has been widely used for the detection of SARS-CoV-2 in the widely known "antigen test" [18-23], this is not the focus of this review.

Zhu et al. [52] proposed a rapid, ultrasensitive, and highly specific assay based on the association of reverse transcription multiple cross displacement amplification (RT-MCDA) with CRISPR-Cas12a-based detection to develop MCCD as novel diagnostic test targeting *ORF1ab* and *N* genes. The MCCD assay can be visualized on a lateral flow biosensor and completed within 1 h including the whole process from the RNA extraction to the detection reaction

and reporting of result. At the isothermal amplification stage of this MCCD lateral flow assay, two sets of MCDA primers, which recognized regions of *ORF1ab* and *N* genes, respectively, ensured the high specificity for SARS-CoV-2 RNA. After the reverse transcription, the final detection associated with CRISPR12a, which specifically recognized predefined target sequences and degradated a ssDNA molecule, allowed the detection of 7 copies per test. Moreover, the feasibility of the proposed assay as a SARS-CoV-2 diagnostic tool was validated using the extracted RNA from clinical samples. **Ali et al.** [53] proposed a biosensing methodology called iSCAN (*in vitro* specific CRISPR-based assay for nucleic acid detection), which combines the target amplification *via* RT-LAMP with CRISPR-Cas12a for the efficient, rapid, specific, and sensitive colorimetric SARS-CoV-2 detection at a level of 10 copies per reaction. iSCAN is a user-friendly methodology since the colorimetric reaction coupled with lateral flow immunochromatography made it easier to interpret the assay results. In addition, iSCAN assay was successfully used in nasopharyngeal swabs of healthy persons and patients with COVID-19. **Zhu et al.** [54] reported the use of a multiplex RT-LAMP coupled to a nanoparticle-based lateral flow biosensor assay (mRT-LAMP-LFB) for diagnosing COVID-19 *via ORF1ab* and *N* genes detection (Fig. 9). After amplification, ORF1ab-RT-LAMP products were simultaneously labeled with fluorescein (FITC) and biotin, and N-RT-LAMP products with digoxin (Dig) and biotin, which were determined by LFB through immunoreactions. At the detection stage, one end of the RT-LAMP products can be captured by anti-FITC or anti-Dig antibodies located in TL1 region or TL2 region, respectively, and the other end labeled with biotin can bind streptavidin-conjugated colored nanoparticles for visualization. The

detection limit of mRT-LAMP-LFB was 12 copies (for each detection target) per reaction, and no cross-reactivity was observed with non-SARS-CoV-2 templates. Moreover, both its sensitivity and specificity were 100% for the detection of SARS-CoV-2 in oropharynx swab samples collected from COVID-19 patients and non-COVID-19 patients, respectively. **Wang et al.** [55] pioneered the development and application of an inexpensive amplification-free nucleic acid immunoassay based on LF assays for the fluorescence detection of *ORF1ab*, *E* and *N* genes of the SARS-CoV-2 genome in less than one hour, which was called hybrid capture-fluorescence immunoassay (HC-FIA). The authors used fluorescent nanoparticles composed of europium chelate (FNPs) labelled with S9.6 monoclonal antibodies to bind with high affinity and selectivity to the RNA-DNA hybrid formed by the designed DNA probes and the RNA of SARS-CoV-2 on LF strip. The HC-FIA assay showed a detection limit of 500 copies of target genes per mL and achieved sensitivities of 100% and specificities of 99% for both throat swabs and sputum samples. Moreover, the portable device for fluorescence signal reading can meet the requirements of POC technology.
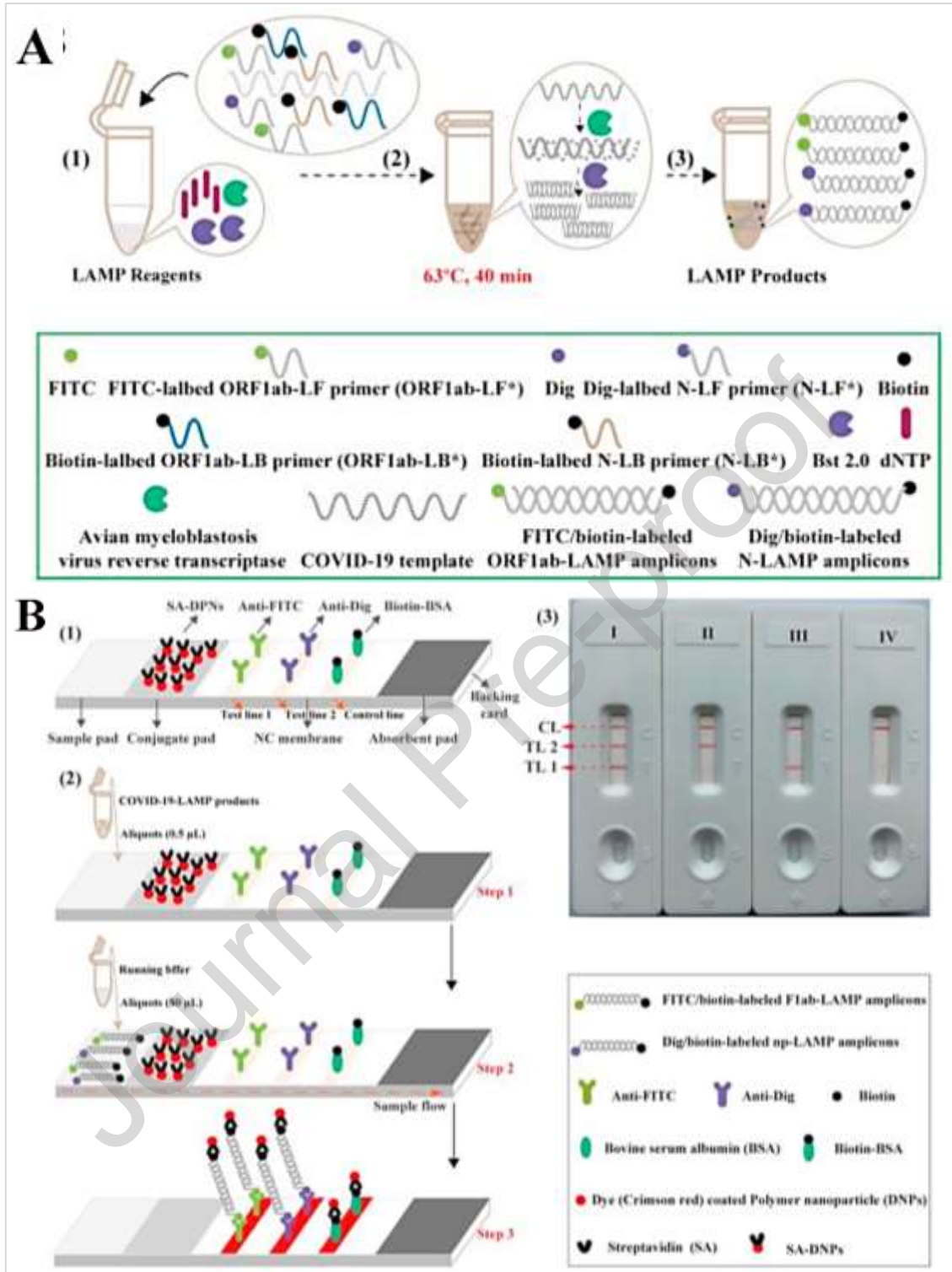
Fig. 9. Schematic representation of the mRT-LAMP-LFB assay for diagnosing COVID-19 *via ORF1ab* and *N* genes detection. (A) Mechanistic description of the mRT-LAMP: (1) preparing the amplification mixtures, (2) RT-LAMP reaction, and (3) the detectable COVID-19 RT-LAMP products after reaction. (B)

Principle of LFB for visualization of COVID-19 RT-LAMP products: (1) the details of LFB, (2) the principle of LFB for COVID-19 RT-LAMP products, and (3) the interpretation of the COVID-19 RT-LAMP results. I. a positive result for *ORF1ab* and *N* genes (TL1, TL2, and control line appear on the LFB); II. a positive result for N-gen (TL2 and control line appear on the detection region); III. a positive result for *ORF1ab* gen (TL1 and control line appear on the detection region); IV. negative (only the control line appears on the LFB). Adapted from Ref. [54], Copyright (2020), with permission from Elsevier.

Nguyen et al. [56] proposed an interesting wearable freeze-dried, cell-free (FDCF) general sensor with successful application for SARS-CoV-2 RNA detection. They developed a face-mask that collects the virus as a consequence of coughing, talking or normal respiration. The mask-sensor contains four main components: an hydration reservoir, a collection pad, a microfluidic paper-based analytical device (μpad) and a LF-strip. By capillary action, the viral particles are moved from the collection pad to the μpad which is organized in different reaction zones separated by polyvinyl alcohol. In these regions take place the lysis of viral membrane, the RT-RPA reaction and the detection of the amplified dsDNA amplicon through the Cas12a SHERLOCK sensor. In the presence of SARS-CoV-2-derived amplicons, the activated Cas12a enables *trans*-cleavage of a co-lyophilized 6-FAM-(TTATTATT)-biotin ssDNA probe to allow a simple colorimetric visual readout at the LF strip. The global process takes approximately 1.5h at room temperature and presents a detection limit of 500 copies.

Currently, the *in vitro* assays integrating nucleic acids amplification techniques with LF are commercially available for diagnostic test of SARS-CoV-2. The Accula SARS-CoV-2 Test (Mesa Biotech, now ThermoFisher) is a PCR NAAT that allows a hybridization-based visual detection of viral RNA in 30 min using a completely automated and self-contained system, although it requires a dock that controls reaction temperatures, timing, and fluid movements within the test cassette [57,58]. The COVID-19 RNA Test (PortNAT System, USTAR BIOTECHNOLOGIES) is carried out in an all-in-one test cassette with a reusable incubator, which uses isothermal cross-priming amplification (CAP) and takes 35 min for the amplification and 5 min for reading the results in the LF strip [59,60]. The Veros COVID-19 Test (Sense Biodetection) is a disposable automated device covered by patents, which *via* nucleic acid amplification allows to obtain results in about 15 min. This single-use test contains all the reagents, enzymes, and detection strip required to perform an assay, but it needs to be powered with 1.5 V DC battery [61, 62]. In addition, the HC-FIA developed by Wang et al. [55], has been approved by the National Medical Products Administration of China (registration number, 20203400298) and acquired the European Conformity (registration number, NL-CA002-2020-50112).

Table 1. Comparison of the analytical performance of the most relevant biosensing strategies developed for SARS-CoV-2 RNA detection.

Biosensing with electrochemical transduction						
Detection Technique	Electrode	Platform	Linear Range	Detection Limit	Sample	Ref.
Amperometry	SPAuE	Thiolated capture	0 - 80 pM	0.6 pM	SARS-CoV-2	[28

		probe immobilized on maleimide-coated magnetic beads. Amplification system employing a sandwich-type scheme based on STP-HRP conjugates.			cell culture	
EIS	GCE	Biotinylated probe sequence immobilized on a MWCNTs-Av hybrid as biocapture nanoplatform	1.0×10^{-18} M - 1.0×10^{-11} M	0.33 aM	Samples obtained from SARS-CoV-2 RNA PCR	[29
DPV	SPAuE	Mixture of different shape Au nanostructures to immobilize a thiolated DNA probe sequence combined with MB-functionalized carbon nanodots	10.0 aM - 10.0 nM	2.2 aM	Nasopharyngeal samples of COVID-19 patients	[30
DPV	SPCE	SPCE modified BNQDs and FGNs as anchoring site for a thiolated DNA probe	1.0×10^{-18} M - 1.0×10^{-9} M	0.27 aM	Nasopharyngeal swabs of healthy subjects and COVID-19 patients	[31
V $versus$ t measurments	Au	Graphene suspension as a support for ssDNA probes-capped AuNPs	585.4 copies/µL - 5.854×10^{7} copies/µL	6.9 copies/µL	Clinical samples from COVID-19 patients and healthy asymptomatic subjects	[32
EDL-gated BioFET	Au	Thiolated ssDNA probes immobilized on sensor surface	1 fM - 1 pM	< 1 fM	Saliva	[33
DPV	Au	Target-triggered cascade signal amplification by integration of CHA and TdT, and using $[Ru(NH_3)_6]^{3+}$ electrostatically adsorbed as redox marker	0.1 pM - 3000 pM	45 fM	Oropharyngeal swabs of healthy subjects and COVID-19 patients	[34
DPV	Au	Target-triggered cascade signal amplification by integration of CHA, target recycling, Y-shaped DNA structure formation, and TdT, and using $[Ru(NH_3)_6]^{3+}$ electrostatically adsorbed as redox marker	0.1 pM - 1000 pM	26 fM	Oropharyngeal swabs of healthy subjects and COVID-19 patients	[35

31

Detection Technique	Electrode	Working principle	Linear Range	Detection Limit	Sample	Ref.
SWV	SPAuE	Graphene as a support for MECS based on DNA nanostructures mimicking a hydra architecture. Tentacle contains the DNA probe and MB as electrochemical label.	0.05 copies/µL - 500 copies/µL	4 copies/ 80 µL	Nasopharyngeal swabs	[36

Biosensing with electrochemiluminescence transduction						
Detection Technique	**Electrode**	**Working principle**	**Linear Range**	**Detection Limit**	**Sample**	**Ref.**
ECL	Au	DNA tetrahedron immobilized on electrode surface contains the ssDNA capture probe that enables the target DNA-participated entropy-driven amplified reaction and leads to linking of the $[Ru(bpy)_3]^{2+}$-modified DNA to the exposed domain of the capture probe to give "ECL on"	1 fM - 100 pM	2.67 fM	Human serum	[37
Dual-wavelength ratiometric ECL	Au	RET mechanism between $g\text{-}C_3N_4$, linked to a triple helix DNA, and Ru-SiO_2@FA, bridged to upright DNA on $g\text{-}C_3N_4$ via output DNA, combined with 3D DNA walker amplification that converted a trace amount of target into a large number of output DNA	1 fM - 10 nM	0.18 fM	Healthy human throat swabs	[38
Dual-wavelength ratiometric ECL	GCE	RET mechanism between $Au\text{-}g\text{-}C_3N_4$, linked to TDNAs with a hairpin structure as walking tracks for the bipedal DNA walker, and PEI-$Ru@Ti_3C_2$@AuNPs-DNA7, used to combine with the excised hairpin part of TDNAs, based on both target-triggered entropy-driven and bipedal DNA walker amplification strategies	10 aM - 10 pM	7.8 aM	Human serum	[39
Dual-wavelength ratiometric ECL	GCE	RET mechanism between $Au\text{-}g\text{-}C_3N_4$, bound to a DNA that can pair with a part of	Up to 30 fM	59 aM	Normal human pharyngeal swabs	[40

32

Detection Technique	Working principle	Linear Range	Detection Limit	Sample	Ref.
ECL	GCE	target (DNA1), and $[Ru(bpy)_3]^{2+}$, linked to another DNA probe (Ru1), based on HCR amplification induced by a Y-DNA probe linked to hairpins and Ru1. One part of target can pair with DNA1 and the other part with the Y-type probe and open the hairpin structure.			

(continued)

| ECL | GCE | Activation of the cleavage activity of CRISPR-Cas12a using dsDNA amplified from target DNA by a 3D DNA walker. PEI-Ru@Ti$_3$C$_2$@AuNPs-DNA7-based ECL signal increases when activated CRISPR-Cas12a cleaves Fc-modified ssDNA7 causing Fc (quencher) to move away from electrode surface. | Up to 500 aM | 12.8 aM | Pharyngeal swab | [41 |

Biosensing with optical transduction

Detection Technique	Working principle	Linear Range	Detection Limit	Sample	Ref.
Naked-eye and smartphone-based colorimetric detection	Target-derived dsDNA amplicons trigger the CRISPR-Cas12a-based degradation of a linker ssDNA of two AuNPs-DNA probes, inducing the AuNPs disaggregation and generating observable color changes	10^0 - 10^8 copies/µL.	1.0 copy/µL	Positive and negative clinical swab samples	[43
Personal glucose meter	Target-derived dsDNA amplicons trigger the CRISPR-Cas12a-based degradation of a linker ssDNA between invertase and MBs, releasing invertase from residual MBs by magnetic separation which catalyzes the conversion of sucrose to glucose	10^1 - 10^4 copies/µL	10 copies/µL	Clinical samples of healthy subjects and COVID-19 patients	[44
Raman spectroscopy	Target-derived dsDNA amplicons trigger the CRISPR-Cas12a-based degradation of a SERS probe formed by MBs and AgNPs@4-ATP linked through a linker ssDNA, removing the Raman tags of the MBs and thus decreasing the Raman intensity	---	1.0 fM	Nasopharyngeal swabs	[45
Naked-eye and colorimetric detection	Target RNA triggers the CRISPR-Cas13a-based cleavage of ssRNA oligonucleotides conjutaded to AuNPs, inducing their colloidal aggregation and generating observable color changes	---	100 pM	Nasopharyngeal swabs	[46

33

Fluorescence	CRISPR-mCas13 recognizes and cleaves RT-LAMP-amplified target RNA sequences, exhibiting collateral cleavage activity that degrades a ssRNA reporter (formed by a fluorophore, a short ssRNA sequence, and a quencher), which emits fluorescence upon cleavage of the short ssRNA	---	4.0 copies/µL	Oropharyngeal and nasopharyngeal swabs	[47
Fluorescence	Molecular beacon based on ht-G3 lights up Thioflavin T in potassium solution, whose fluorescente increases significantly after adding the target RNA. DSN was introduced for target recycling and signal amplification.	0.1 nM - 1.0 nM	0.01 nM	---	[48
Naked-eye detection based on µPAD	*in situ* formation of anisotropic AuNPs using ASOs and a polyG tail, which after hybridization with target RNA undergo aggregation and generate observable color change	---	---	Throat samples	[49

Lateral Flow biosensing					
Detection Technique	Working principle / Platform	Linear Range	Detection Limit	Sample	Ref.
LFB	Target-derived dsDNA amplicons obtained by RT-MCDA trigger the CRISPR-Cas12a-based cleavage of FITC/biotin-labeled ssDNA reporters. STP-AuNPs deposited on the conjugate region and Anti-FITC and bBSA as the capture reagents on control line and test line, respectively.	---	7 copies per test	Swabs	[52
LFB	Target-derived dsDNA amplicons obtained by RT-LAMP trigger the CRISPR-Cas12a-based cleavage of fluorophore/quencher-labeled ssDNA reporters.	---	10 copies per reaction	Nasopharyngeal swabs	[53
LFB	Two different target-derived dsDNA amplicons obtained by RT-LAMP were simultaneously labeled, one with FITC and biotin and another Dig and biotin. STP-DNPs deposited on the conjugate region and Anti-FITC (test line), Anti-Dig (test line), and bBSA (control line) as the capture reagents on the detection region.	---	12 copies per reaction	Oropharynx swab samples	[54
LFB	FNPs labelled with S9.6 monoclonal antibodies capture the RNA target-DNA probe hybrid. S9.6 monoclonal antibodies and Anti-rabbit IgG polyclonal antibodies prefixed on test line and control line, respectively.	---	500 copies/mL	Throat swabs and sputum samples	[55]
LFB	Face-mask sensor with collection of the sample in the inner part of a mask, and sensing following	---	500 copies/mL	----	[56]

34

different steps: lysis , RT-RPA amplification at room temperature,and detection by CAS12a that results in collateral cleavage of FAM-biotin ssDNA probes, and LF detection through the use of anti-FAM conjugated AuNPs.	

Abbreviations: SPAuE: screen-printed gold electrodes; STP: streptavidin; HRP: horseradish peroxidase; EIS: electrochemical impedance spectroscopy; GCE: glassy carbon electrode; MWCNTs: multi-walled carbon nanotubes; Av: avidin; RNA: ribonucleic acid; PCR: polymerase chain reaction; DPV: differential pulse voltammetry; DNA: deoxyribonucleic acid; MB: methylene blue; SPCE: screen-printed carbon electrodes; BNQDs: boron nitride quantum dots; FGNs: flower-like gold nanostructures; ssDNA: single-stranded deoxyribonucleic acid; AuNPs: gold nanoparticles; EDL-gated BioFET: electrical double layer-gated field-effect transistor-based biosensor; CHA: catalytic hairpin assembly; TdT: terminal deoxynucleotidyl transferase; SWV: square wave voltammetry; MECS: self-actuator molecular-electrochemical system; ECL: electrochemiluminescence; $[Ru(bpy)_3]^{2+}$: tris(4,4′-dicarboxylic acid-2,2′-bipyridyl)ruthenium(II); RET: resonance energy transfer; g-C_3N_4: graphitic carbon nitride nanosheets; Ru-SiO_2@FA: Ru-SiO_2 nanospheres functionalized with folic acid; Au-g-C_3N_4: graphite-C_3N_4 decorated with AuNPs; PEI-Ru@Ti_3C_2@AuNPs-DNA7: Nanocomposite of polyethylenimine, $Ru(bpy)_3^{2+}$, Ti_3C_2 MXene, gold nanoparticles, and thiolated DNA probe; HCR: hybridization chain reaction; Y-DNA: three-stranded Y-type DNA; CRISPR-Cas12a: clustered regularly interspaced short palindromic repeats-associated protein 12a; dsDNA: double-stranded deoxyribonucleic acid; Fc: ferrocene; MBs: magnetic beads; SERS: surface-enhanced Raman spectroscopy; AgNPs@4-ATP: silver nanoparticles modified with 4-aminothiophenol; CRISPR-Cas13a: CRISPR-associated endonuclease LwaCas13a; ssRNA: single-stranded ribonucleic acid; CRISPR-mCas13: CRISPR-associated miniature Cas13; RT-LAMP: reverse transcription loop-mediated isothermal amplification; µPAD: microfluidic paper-based analytical device; ASOs: antisense oligonucleotides; PolyG: polyguanine; LFB: lateral flow biosensor; RT-MCDA: reverse transcription multiple cross displacement amplification; FITC: fluorescein; Anti-FITC: rabbit antifluorescein antibody; bBSA: biotinylated bovine serum albumin; Dig: digoxin; DNPs: dye-coated polymer nanoparticles; Anti-Dig: sheep antidigoxin antibody; FNPs: fluorescent nanoparticles composed of europium chelate;

3. Conclusion and future outlook

The fast, friendly, sensitive, and selective detection of SARS-CoV-2 is highly required for the early diagnosis of COVID-19. The negative impact of the COVID-19 outbreak on health systems all around the world was the engine for the development of different biosensing strategies. RT-PCR, the gold standard technique, has demonstrated to be extremely useful during the most critical period of the pandemic; however, it presents several limitations connected to the problem of the false negative for infected people with low level of virus and the difficulties for descentralized use. Three years after the beginning of the COVID-19 pandemic, in addition to RT-PCR, we have a battery of sensing

methodologies that allowed us to obtain information at the different stages of the disease, either to confirm the presence of the virus (viral RNA or viral protein), at the first days, mainly based on isothermal amplification, or to know the immunological response of the host due to the presence of the virus (immunoglobulins) after the first week.

Biosensors represent an interesting alternative for the quantification of SARS-CoV-2 nucleic acid, either associated to isothermal amplification strategies following different transduction schemes, or without amplification, mainly in the case of electrochemical transduction. In this sense, the known advantages of electrochemical biosensors, connected with the possibility of miniaturization, friendly use, high sensitivity and selectivy and fast response, make them an interesting alternative for the direct quantification of SARS-CoV-2 nucleic acid, either by developing new devices or or even taking advantage of the well-known portable glucometers.

The combination of adequate extraction and amplification strategies with LF-immunosensig readout, has allowed the highly sensitive and selective detection of SARS-CoV-2 RNA, with successful applications in the market, representing a very promising biosensing alternative for POC measurements. The association of the LF with the biosensing principles have already proven to be extremely useful for large-scale manufacturing. In fact, the mass production of the well-known "antigen test", their sale in pharmacies, and their use by patients at home without need to attend to the hospitals or screening centers, undoubtedly represented a before and after in the diagnosis of COVID-19 and made possible a significant decompression of the collapsed healthcare systems around the world, even when it is not sensitive enough during the first days of the COVID-

19. Based on these excellent results, is expected that LF biosensors for the detection of viral RNA or viral particles be also successful and allow an early, sensitive and fast POC diagnostic of COVID-19.

However, in spite of the advantages of these excellent diagnostic tools, the development of massive biosensors for the detection/quantification of SARS-CoV-2 RNA with the sensitivity enough to detect the presence of RNA at very early stages of the COVID-19, is still one important challenge. Thus, the "to do list" for the future of SARS-CoV-2 biosensing platforms involves the development of fast, accurate, amplification-free, and large-scale multiplex POC devices for SARS-CoV-2 RNA quantification with a sensitivity high enough to detect very low number of copies and new mutations of the virus.

Declaration of Competing Interest

On behalf of the authors of the review "Biosensing strategies for the detection of SARS-CoV-2 nucleic acids" by Tamborelli, López Mujica, Gallay, Vaschetti, Reartes, Del Pino, Bravo, Bollo, Rodríguez, Rubianes, Dalmasso, and Rivas, we declare that there are no conflicts of interest. Graphical abstract has been created using assets from Freepik.com and with the aid of Servier Medical Art by Servier (licensed under a Creative Commons Attribution 3.0 Unported License).

Acknowledgements

References

[1] C. Li, C. Zhao, J. Bao, B. Tang, Y. Wang, B. Gu, Laboratory diagnosis of coronavirus disease-2019 (COVID-19), Clin. Chim. Acta 510 (2020) 35-46.

[2] World Health Organization, https://www.who.int/publications/m/item/weekly-epidemiological-update-on-covid-19---1-march-2023, 2023 (accessed 6 March 2023).

[3] D.K.W. Chu, Y. Pan, S.M.S. Cheng, K.P.Y. Hui, P. Krishnan, Y. Liu, D.Y. M. Ng, C.K.C. Wan, P. Yang, Q. Wang, M. Peiris, L.L.M. Poon, Molecular diagnosis of a novel coronavirus (2019-nCoV) causing an outbreak of pneumonia, Clin. Chem. 66 (2020) 549-555.

[4] A. Sharma, K. Kontodimas, M. Bosmann, Nanomedicine: a diagnostic and therapeutic approach to COVID-19, Front. Med. 8 (2021) 648005.

[5] J.F. Drexler, F. Gloza-Rausch, J. Glende, V.M. Corman, D. Muth, M. Goettsche, A. Seebens, M. Niedrig, S. Pfefferle, S. Yordanov, L. Zhelyazkov, U. Hermanns, P. Vallo, A. Lukashev, M.A. Müller, H. Deng, G. Herrler, C. Drosten, Genomic characterization of severe acute respiratory syndrome-related

coronavirus in European bats and classification of coronaviruses based on partial RNA-dependent RNA polymerase gene sequences, J. Virol. 84 (2010) 11336-11349.

[6] E. de Wit, N. van Doremalen, D. Falzarano, V.J. Munster, SARS and MERS: recent insights into emerging coronaviruses, Nat. Rev. Microbiol. 14 (2016) 523-534.

[7] Coronaviridae Study Group of the International Committee on Taxonomy of Viruses, The species severe acute respiratory syndrome-related coronavirus: classifying 2019-nCoV and naming it SARS-CoV-2. Nat. Microbiol. 5 (2020) 536-544.

[8] I. Astuti, Ysrafil, Severe acute respiratory syndrome coronavirus 2 (SARS-CoV-2): an overview of viral structure and host response, Diabetes Metab. Syndr. 14 (2020) 407-412.

[9] A.R. Fehr, S. Perlman, Coronaviruses: an overview of their replication and pathogenesis, Coronaviruses 1282 (2015) 1-23.

[10] B. Coutard, C. Valle, X. De Lamballerie, B. Canard, N.G. Seidah, E. Decroly, The spike glycoprotein contains a furin-like cleavage site absent in CoV of the same clade, Antiviral Res. 176 (2020) 104742.

[11] S. Perlman, Another decade, another coronavirus. N. Engl. J. Med. 382 (2020) 760-762.

[12] F. Sanchis-Gomar, C.J. Lavie, C. Perez-Quilis, B.M. Henry, G. Lippi, Angiotensin-converting enzyme 2 and antihypertensives (angiotensin receptor blockers and angiotensin-converting enzyme inhibitors) in coronavirus disease 2019, Mayo Clin. Proc. 95 (2020) 1222-1230.

[13] A. Parasher, COVID-19: current understanding of its pathophysiology, clinical presentation and treatment, Postgrad. Med. J. 97 (2021) 312-320.

[14] K. Yuki, M. Fujiogi, S. Koutsogiannaki, COVID-19 pathophysiology: a review, J. Clin. Immunol. 215 (2020) 108427.

[15] E.S. Goudouris, Laboratory diagnosis of COVID-19, J. Pediatr. 97 (2021) 7-12.

[16] A. La Marca, M. Capuzzo, T. Paglia, L. Roli, T. Trenti, S.M. Nelson, Testing for SARS-CoV-2 (COVID-19): a systematic review and clinical guide to molecular and serological in-vitro diagnostic assays, Reprod. BioMed. Online 41 (2020) 483-499.

[17] A. Aziz, M. Asif, G. Ashraf, U. Farooq, Q. Yang, S. Wang, Trends in biosensing platforms for SARS-CoV-2 detection: a critical appraisal against standard detection tools, Curr. Opin. Colloid. Interface Sci. 52 (2021) 101418.

[18] M. Castellanos, A. Somoza, Emerging clinically tested detection methods for COVID-19, FEBS J. (2023) https://doi.org/10.1111/febs.16469.

[19] A. Rubio-Monterde, D. Quesada-González, A. Merkoçi, Toward integrated molecular lateral flow diagnostic tests using advanced micro- and nanotechnology, Anal. Chem. 95 (2023) 468-489.

[20] L. Tessaro, A. Aquino, P. Panzenhagen, N. Joshi, C.A. Conte-Junior, A systematic review of the advancement on colorimetric nanobiosensors for SARS-CoV-2 detection, J. Pharm. Biomed. Anal. 222 (2023) 115087.

[21] O. Filchakova, D. Dossym, A. Ilyas, T. Kuanysheva, A. Abdizhamil, R. Bukasov, Review of COVID-19 testing and diagnostic methods, Talanta 244 (2022) 123409.

[22] M.J. Oishee, T. Ali, N. Jahan, S.S. Khandker, M.A. Haq, M.U. Khondoker, B.K. Sil, H. Lugova, A. Krishnapillai, A.R. Abubakar, S. Kumar, M. Haque, M.R. Jamiruddin, N. Adnan, COVID-19 Pandemic: review of contemporary and forthcoming detection tools, Infect. Drug Resist. 14 (2021) 1049-1082.

[23] M. Mostafa, A. Barhoum, E. Sehit, H. Gewaid, E. Mostafa, M.M. Omran, M.S. Abdall, F.M. Abdel-Haleem, Z. Altintas, R.J. Forster, Current trends in COVID-19 diagnosis and its new variants in physiological fluids: surface antigens, antibodies, nucleic acids, and RNA sequencing, Trends Analyt. Chem. 157 (2022) 116750.

[24] H. Ledford, E. Callaway, Pioneers of revolutionary CRISPR gene editing win chemistry Nobel. Nature 586 (2020) 346–347.

[25] G.S. Park, K. Ku, S.H. Baek, S.J. Kim, S.I. Kim, B.T. Kim, J.S. Maeng, Development of reverse transcription loop-mediated isothermal amplification (RT-LAMP) assays targeting SARS-CoV-2, J. Mol. Diagn. 22 (2020) 729-735.

[26] Y.H. Baek, J. Um, K.J.C. Antigua, J.-H. Park, Y. Kim, S. Oh, Y. Kim, W.-S. Choi, S.G. Kim, J.H. Jeong, B.S. Chin, H.D.G. Nicolas, J.-Y. Ahn, K.S. Shin, Y.K. Choi, J.-S. Park, M.-S. Songa, Development of a reverse transcription-loop-mediated isothermal amplification as a rapid early-detection method for novel SARS-CoV-2. Emerg. Microb. Infect. 9 (2020) 998–1007.

[27] S.S. Mahshid, S.E. Flynn, S. Mahshid, The potential application of electrochemical biosensors in the COVID-19 pandemic: a perspective on the rapid diagnostics of SARS-CoV-2, Biosens. Bioelectron. 176 (2021) 112905.

[28] S. Cajigas, D. Alzate, M. Fernández, C. Muskus, J. Orozco, Electrochemical genosensor for the specific detection of SARS-CoV-2, Talanta 245 (2022) 123482.

[29] M.L. Mujica, A. Tamborelli, A. Castellaro, D. Barcudi, M.D. Rubianes, M.C. Rodríguez, H.A. Saka, J.L. Bocco, P.R. Dalmasso, G.A. Rivas, Impedimetric and amperometric genosensors for the highly sensitive quantification of SARS-CoV-2 nucleic acid using an avidin-functionalized multi-walled carbon nanotubes biocapture platform, Biosens. Bioelectron. X 12 (2022) 100222.

[30] C. Pina-Coronado, Á. Martínez-Sobrino, L. Gutiérrez-Gálvez, R. Del Caño, E. Martínez-Periñán, D. García-Nieto, M. Rodríguez-Peña, M. Luna, P. Milán-Rois, M. Castellanos, M. Abreu, R. Cantón, J.C. Galán, T. Pineda, F. Pariente, Á. Somoza, T. García-Mendiola, R. Miranda, E. Lorenzo, Methylene Blue functionalized carbon nanodots combined with different shape gold nanostructures for sensitive and selective SARS-CoV-2 sensing, Sens. Actuators B Chem. 369 (2022) 132217.

[31] B. Hatamluyi, M. Rezayi, S. Amel Jamehdar, K.S. Rizi, M. Mojarrad, Z. Meshkat, H. Choobin, S. Soleimanpour, M.T. Boroushaki, Sensitive and specific clinically diagnosis of SARS-CoV-2 employing a novel biosensor based on boron nitride quantum dots/flower-like gold nanostructures signal amplification, Biosens. Bioelectron. 207 (2022) 114209.

[32] M. Alafeef, K. Dighe, P. Moitra, D. Pan, Rapid, ultrasensitive, and quantitative detection of SARS-CoV-2 using antisense oligonucleotides directed electrochemical biosensor chip, ACS Nano 14 (2020) 17028-17045.

[33] A.K. Paulose, C.C. Huang, P.H. Chen, A. Tripathi, P.H. Chen, Y.S. Huang, Y.L. Wang, A rapid detection of COVID-19 viral RNA in human saliva using electrical double layer-gated field-effect transistor-based biosensors, Adv. Mater. Technol. 7 (2022) 2100842.

[34] Y. Deng, Y. Peng, L. Wang, M. Wang, T. Zhou, L. Xiang, J. Li, J. Yang, G. Li, Target-triggered cascade signal amplification for sensitive electrochemical detection of SARS-CoV-2 with clinical application, Anal. Chim. Acta 1208 (2022) 339846.

[35] Y. Peng, Y. Pan, Z. Sun, J. Li, Y. Yi, J. Yang, G. Li, An electrochemical biosensor for sensitive analysis of the SARS-CoV-2 RNA, Biosens. Bioelectron. 186 (2021) 113309.

[36] D. Ji, M. Guo, Y. Wu, W. Liu, S. Luo, X. Wang, H. Kang, Y. Chen, C. Dai, D. Kong, H. Ma, Y. Liu, D. Wei, Electrochemical detection of a few copies of unamplified SARS-CoV-2 nucleic acids by a self-actuated molecular system, J. Am. Chem. Soc. 144 (2022) 13526-13537.

[37] Z. Fan, B. Yao, Y. Ding, J. Zhao, M. Xie, K. Zhang, Entropy-driven amplified electrochemiluminescence biosensor for RdRp gene of SARS-CoV-2 detection with self-assembled DNA tetrahedron scaffolds, Biosens. Bioelectron. 178 (2021) 113015.

[38] T. Yin, Y. Ye, W. Dong, G. Jie, Electrochemiluminescence resonance energy transfer biosensing platform between g-C_3N_4 nanosheet and Ru–SiO_2@FA for dual-wavelength ratiometric detection of SARS-CoV-2 RdRp gene, Biosens. Bioelectron. 215 (2022) 114580.

[39] Z. Fan, B. Yao, Y. Ding, D. Xu, J. Zhao, K. Zhang, Rational engineering the DNA tetrahedrons of dual wavelength ratiometric electrochemiluminescence biosensor for high efficient detection of SARS-CoV-2 RdRp gene by using entropy-driven and bipedal DNA walker amplification strategy, J. Chem. Eng. 427 (2022) 131686.

[40] K. Zhang, Z. Fan, Y. Huang, Y. Ding, M. Xie, M. Wang, Hybridization chain reaction circuit-based electrochemiluminescent biosensor for SARS-cov-2 RdRp gene assay, Talanta 240 (2022) 123207.

[41] K. Zhang, Z. Fan, Y. Huang, Y. Ding, M. Xie. A strategy combining 3D-DNA Walker and CRISPR-Cas12a trans-cleavage activity applied to MXene based electrochemiluminescent sensor for SARS-CoV-2 RdRp gene detection. Talanta 236 (2022) 122868.

[42] S. Xie, C. Qin, F. Zhao, Z. Shang, P. Wang, M. Sohail, X. Zhang, B. Li, A DNA-Cu nanocluster and exonuclease I integrated label-free reporting system for CRISPR/Cas12a-based SARS-CoV-2 detection with minimized background signals, J. Mater. Chem. B 10 (2022) 6107-6117.

[43] L. Ma, L. Yin, X. Li, S. Chen, L. Peng, G. Liu, S. Ye, W. Zhang, S. Man, A smartphone-based visual biosensor for CRISPR-Cas powered SARS-CoV-2 diagnostics, Biosens. Bioelectron. 195 (2022) 113646.

[44] D. Huang, Z. Shi, J. Qian, K. Bi, M. Fang, Z. Xu, A CRISPR-Cas12a-derived biosensor enabling portable personal glucose meter readout for quantitative detection of SARS-CoV-2, Biotechnol. Bioeng. 118 (2021) 1568-1577.

[45] J. Liang, P. Teng, W. Xiao, G. He, Q. Song, Y. Zhang, B. Peng, G. Li, L. Hu, D. Cao, Y. Tang, Application of the amplification-free SERS-based CRISPR/Cas12a platform in the identification of SARS-CoV-2 from clinical samples, J. Nanobiotechnology 19 (2021) 273.

[46] M. López-Valls, C. Escalona-Noguero, C. Rodríguez-Díaz, D. Pardo, M. Castellanos, P. Milán-Rois, C. Martínez-Garay, R. Coloma, M. Abreu, R. Cantón, J.C. Galán, R. Miranda, Á. Somoza, B. Sot, CASCADE: Naked eye-

detection of SARS-CoV-2 using Cas13a and gold nanoparticles, Anal. Chim. Acta 1205 (2022) 339749.

[47] A. Mahas, Q. Wang, T. Marsic, M.M. Mahfouz, A novel miniature CRISPR-Cas13 system for SARS-CoV-2 diagnostics, ACS Synth. Biol. 10 (2021) 2541-2551.

[48] S. Qin, X. Chen, Z. Xu, T. Li, S. Zhao, R. Hu, J. Zhu, Y. Li, Y. Yang, M. Liu, Telomere G-triplex lights up Thioflavin T for RNA detection: new wine in an old bottle, Anal. Bioanal. Chem. 414 (2022) 6149-6156.

[49] Y.S. Borghei, H.R. Samadikhah, S. Hosseinkhani, Exploitation of N-gene of SARS-CoV-2 to develop a new rapid assay by ASOs@AuNPs, Anal. Chem. 94 (2022) 13616-13622.

[50] V.-T. Nguyen, S. Song, S. Park, C. Joo, Recent advances in high-sensitivity detection methods for paper-based lateral-flow assay, Biosens. Bioelectron. 152 (2020) 112015.

[51] B. Ince, M.K. Sezgintürk, Lateral flow assays for viruses diagnosis: up-to-date technology and future prospects, Trends Analyt. Chem. 157 (2022) 116725.

[52] X. Zhu, X. Wang, S. Li, W. Luo, X. Zhang, C. Wang, Q. Chen, S. Yu, J. Tai, Y. Wang, Rapid, ultrasensitive, and highly specific diagnosis of COVID-19 by CRISPR-based detection, ACS Sens. 6 (2021) 881-888.

[53] Z. Ali, R. Aman, A. Mahas, G.S. Rao, M. Tehseen, T. Marsic, R. Salunke, A.K. Subudhi, S.M. Hala, S.M. Hamdan, A. Pain, F.S. Alofi, A. Alsomali, A.M. Hashem, A. Khogeer, N.A.M. Almontashiri, M. Abedalthagafi, N. Hassan, M.M. Mahfouz, iSCAN: an RT-LAMP-coupled CRISPR-Cas12 module for rapid, sensitive detection of SARS-CoV-2, Virus Res. 288 (2020) 198129.

[54] X. Zhu, X. Wang, L. Han, T. Chen, L. Wang, H. Li, S. Li, L. He, X. Fu, S. Chen, M. Xing, H. Chen, Y. Wang, Multiplex reverse transcription loop-mediated isothermal amplification combined with nanoparticle-based lateral flow biosensor for the diagnosis of COVID-19, Biosens. Bioelectron. 166 (2020) 112437.

[55] D. Wang, S. He, X. Wang, Y. Yan, J. Liu, S. Wu, S. Liu, Y. Lei, M. Chen, L. Li, J. Zhang, L. Zhang, X. Hu, X. Zheng, J. Bai, Y. Zhang, Y. Zhang, M. Song, Y. Tang, Rapid lateral flow immunoassay for the fluorescence detection of SARS-CoV-2 RNA, Nat. Biomed. Eng. 4 (2020) 1150-1158.

[56] Nguyen P.Q., Soenksen L. R., Donghia N. M., Angenent-Mari N. M., De Puig H., Huang A., Lee R., Slomovic S:, Galbersanini T., Lansberry G., Sallum H. M., Zhao E., Niemi J. B., Collins J., V, Nature communication 39 (2021) 1366-1374.

[57] Accula SARS-CoV-2 Test, https://www.fishersci.com/shop/products/accula-sars-cov-2-test-kit/COV4100, 2023 (accessed 24 February 2023).

[58] Accula SARS-CoV-2 Test - Instructions for Use, https://www.fda.gov/media/136355/download, 2023 (accessed 24 February 2023).

[59] PortNAT System, https://en.bioustar.com/product/155.html, 2023 (accessed 28 February 2023).

[60] COVID-19 RNA Test, https://en.bioustar.com/product/151.html, 2023 (accessed 28 February 2023).

[61] Veros COVID-19 Test, https://sense-bio.com/veros-covid-19/, 2023 (accessed 2 March 2023).

[62] Veros COVID-19 Test - Instructions for Use, https://sense-bio.com/wp-content/uploads/Veros-COVID-19-Instructions-for-Use-CD0004-SP-108-v2.0_WEB-1.pdf, 2023 (accessed 2 March 2023).

Authorship contribution statement

Alejandro Tamborelli: Bibliographic search, Formal analysis of the manuscripts**, Michael López Mujica:** Bibliographic search, Formal analysis of the manuscripts**, Pablo Gallay:** Bibliographic search, Formal analysis of the manuscripts**, Virginia Vaschetti:** Bibliographic search, Formal analysis of the manuscripts**, Daiana Reartes:** Bibliographic search, Formal analysis of the manuscripts**, Rocío Delpino;** Bibliographic search, Formal analysis of the manuscripts**, Leonardo Bravo:** Bibliographic search, Formal analysis of the manuscripts**, Soledad Bollo;** Bibliographic search, Formal analysis of the manuscripts**, Conceptualization, Marcela Rodríguez:** Bibliographic search, Formal analysis of the manuscripts**, Conceptualization, María Dolores Rubianes:** Bibliographic search, Formal analysis of the manuscripts**, Conceptualization, Pablo Dalmasso:** Bibliographic search, Formal analysis of the manuscripts**, Conceptualization, Resources, Writing original draft, Writing-review & editing; Funding acquisition**, Gustavo Rivas:** Bibliographic search, Formal analysis of the manuscripts**, Conceptualization, Resources, Writing original draftWriting-review & editing; Funding acquisition

Declaration of interests

47

☒ The authors declare that they have no known competing financial interests or personal relationships that could have appeared to influence the work reported in this paper.

☐The authors declare the following financial interests/personal relationships which may be

considered as potential competing interests:

Graphical abstract:
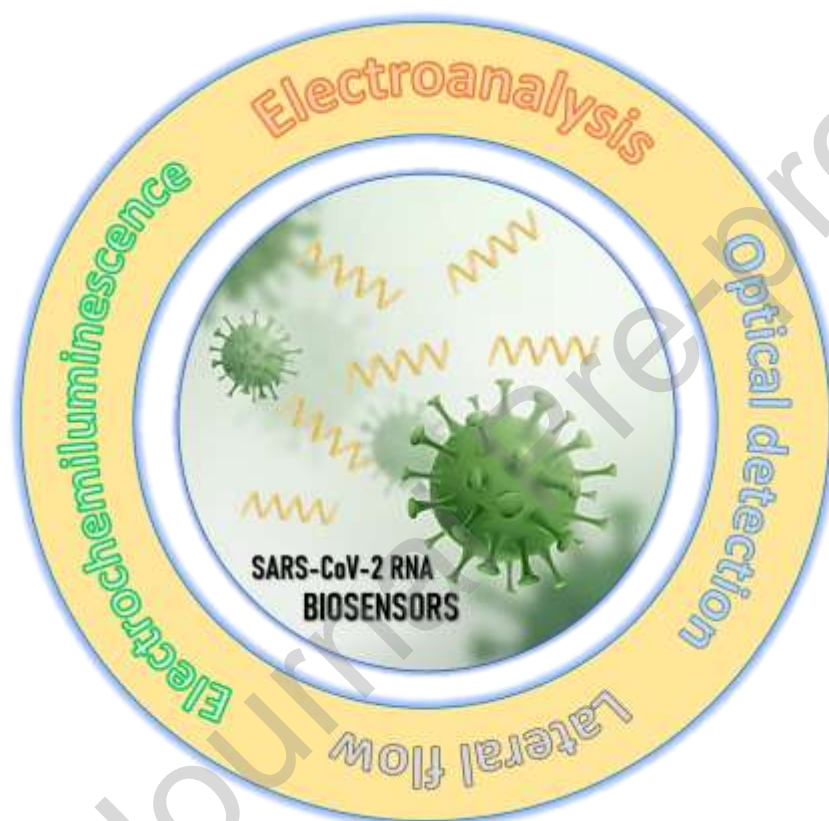
HIGHLIGHTS

- Biosensors have demonstrated to be an excellent analytical tool to quantify SARS-CoV-2.
- Electrochemical genosensors have allowed the sensitive detection of SARS-CoV-2 nucleic acids using simple transduction schemes.
- Isothermal amplification/biosensors association represents an interesting alternative for detecting SARS-CoV-2 nucleic acids.
- Isothermal amplification/Lateral Flow association is an interesting alternative for POC designs.